

## CFD Modelling of Wake-Induced Vibration At Low Reynolds Number

Muhammad Ridhwaan Hassim<sup>1</sup>, Mohd Azan Mohammed Sapardi<sup>1,\*</sup>, Nur Marissa Kamarul Baharin<sup>1</sup>, Syed Noh Syed Abu Bakar<sup>1</sup>, Muhammad Abdullah<sup>1</sup>, Khairul Affendy Mohd Nor<sup>2</sup>

<sup>1</sup> Department of Mechanical Engineering, Kulliyah of Engineering, International Islamic University Malaysia, Jalan Gombak, 53100, Selangor, Malaysia

<sup>2</sup> Department of Mechatronics Engineering, Kulliyah of Engineering, International Islamic University Malaysia, Jalan Gombak, 53100, Selangor, Malaysia

### ARTICLE INFO

#### Article history:

Received 14 August 2021

Received in revised form 11 October 2021

Accepted 12 October 2021

Available online 20 November 2021

#### Keywords:

flow-induced vibration (FIV); wake-induced vibration (WIV); vortex-induced vibration (VIV); Reynolds number; Strouhal number; lift coefficient

### ABSTRACT

Flow-induced vibration is an enthralling phenomenon in the field of engineering. Numerous studies have been conducted on converting flow kinetic energy to electrical energy using the fundamental. Wake-induced vibration is one of the configurations used to optimise the generation of electricity. The results of the study on the effect of the gap between the multiple bluff bodies will provide insight into optimising the energy harvesting process. This study focuses on fluid behaviour and response behind two circular cylinders arranged in tandem when interacting with a fluid flow at low Reynolds numbers ranging from 200 to 1000. The study has been done on several gap lengths between the two cylinders, between  $2D$  and  $5D$ . The study was carried out numerically by using *OpenFOAM*. At  $Re = 1000$ , it is found that the gap length of  $2.5D$  is optimal in terms of producing the highest lift force coefficient on the downstream circular cylinder.

## 1. Introduction

The study of flow-induced vibration (FIV) has been done extensively for the past several years. The study on this area became significant and widespread due to the rapid development of slender or thin structures in modern construction. The interplay between both structure and flow is an exciting problem in engineering mechanics [1]. A vibrating of thin or a very long structure is very natural. However, the galloping and periodic oscillation could cause wear and tear to the structure over a long time. The damage can be worse if the vibration, to some extent, becomes aggressive and responsive. The amplitude of the vibration can be enormous and brings demise to the structure in seconds. This phenomenon is called resonance, where the vibrating frequency coincides with the structure's natural frequency [2]. The resonance phenomenon is often related to the famous incident, the Tacoma Narrow Suspension Bridge collapse in 1940. A study conducted by Irwin *et al.*, [3] established the factors of the incident and design of the new bridge structure. Aerodynamic instability is the main principle of the problem, which triggers many efforts to solve the problem. The

\* Corresponding author.

E-mail address: [azan@iium.edu.my](mailto:azan@iium.edu.my) (Mohd Azan Mohammed Sapardi)

<https://doi.org/10.37934/cfdl.13.11.5364>

flow-induced vibration (FIV) study problems are currently simplified to free-flowing fluid in an open channel interacting with bluff bodies. Investigation on this simplified model can provide a reasonable interpretation of the problem's pressure, fluid force distribution, and vortex dynamic [4].

Flow-induced vibration (FIV) can be in two forms which are vortex-induced vibration (VIV) and wake-induced vibration (WIV). The induced vibration on a single isolated rigid cylinder with an incoming linear flow to the bluff body is known as VIV. Many researchers have studied VIV, such as Naseer *et al.*, [5], Pinar *et al.*, [6], Soti *et al.*, [7], Zahari and Dol [8] and Atrah *et al.*, [9]. On the other hand, vibration can also be induced on a bluff body that experiences the wake of a flow from another bluff body known as WIV. The two cylinders, or more, can be arranged in tandem or staggered, such as in studies by Assi [10] and Assi *et al.*, [11].

Based on a study made by Zhang and Wang [12], reducing the velocity, therefore the Reynolds number, affects the amplitude response of the cylinder. There is an optimal Reynolds value where the amplitude is at the peak, indicating a resonance. Another study from Soti *et al.*, [7] also reaches a similar conclusion where the amplitude response is highest at a particular value of Reynolds.

The wake mode or pattern of the vortex is commonly described in many papers. The study of wake mode involves observing the vortices shed at alternating sides of the bluff body. Many variables influence the formation of different modes, such as inlet velocity of flow and the gap length between cylinders. The famous Karman Vortex Street is the two singles (2S) mode where one single vortex is formed at each alternating side of the wake region. Blackburn and Henderson [13] and Soti *et al.*, [7] also observed 2S mode at lock-in regions where the flow is laminar in their free cylinder vibration experiments. Atrah *et al.*, [9] also reported the formation of 2S mode when the amplitude is at the peak, where lock-in occurs. In their report, they found that there is a critical diameter to achieve the highest amplitude. By varying the ratio between the frequency of oscillation and the vortex shedding frequency, Fu *et al.*, [14] observed two pair (2P) mode where the lift force shows periodic harmonic characteristics, indicating the lock-in phase. A study of forced cylinder vibration by Singh and Biswas [15] observed multiple modes of vortex shedding, which are 2S, 2P and single (P + S) modes appear in the wake region for various setups of their study.

A significant amount of effort was focused on developing energy harvesters to extract energy from a free-flowing fluid. The step taken on this effort is crucial as finite resources will continue to deplete; thus, harnessing renewable and clean energy is still a focal point. Converting fluid energy to electrical energy covers a wide operating range, for example, extracting power from wind energy and hydro energy [16,17]. Examples of undergoing research that can be found are harvesting flow energy using a piezoelectric energy harvester, electromagnetic damping and slender belt [7,9,12,17,18]. From Atrah *et al.*, [9], the energy is collected from the physical amplitude motion of the cylinder. The amount of energy harvested is directly proportional to the amplitude response of the cylinder. Hence, it is crucial to find the relationship between the characteristic length, which is, in most cases, are the diameter of the cylinder, the velocity of the fluid, and the gap between the cylinders onto the lift force coefficient and the frequency. This could give a good insight into future works in designing the correct setup for the WIV system.

This study is motivated by the application of the wake-induced-vibration in energy harvesting. However, this study focuses on the fundamental effect of low Reynolds number on the wake frequency in an external flow with two circular cylinders in a tandem arrangement. The effects of low Reynolds number and gap length on the response amplitude and lift coefficient on the downstream cylinder are studied. Finally, an optimal gap length that gives the highest amplitude response within the range of the studied parameter is determined.

## 2. Methodology

The flow is assumed to be incompressible that is governed by Navier-Stokes's equations:

$$\nabla \cdot \mathbf{u} = 0 \quad (1)$$

$$\frac{\partial \mathbf{u}}{\partial t} + (\mathbf{u} \cdot \nabla) \mathbf{u} = -\nabla p + \frac{1}{Re} (\nabla^2 \mathbf{u}) \quad (2)$$

where  $\mathbf{u}$  represents the velocity field,  $t$  represents time,  $p$  represents the kinematic pressure, and  $Re$  represents the Reynolds number that is defined as,

$$Re = \frac{\rho U D}{\mu} = \frac{U D}{\nu} \quad (3)$$

where  $\rho$  represents the fluid density,  $\mu$  represents the dynamic viscosity,  $\nu$  represents the kinematic viscosity,  $U$  represents the free stream velocity, and  $D$  represents the diameter of the cylinder.

The Strouhal number, representing the dimensionless value of the vortex shedding frequency from the cylinder, is determined by using,

$$St = \frac{f_v D}{U} \quad (4)$$

where  $f_v$  is the frequency of vortex shedding.

*OpenFOAM* is an open-source software to simulate the fluid dynamics of a system. An incompressible and laminar flow solver is used for the simulation.

### 2.1 Geometry and Physical Descriptions

The present study has two geometry setups; a single cylinder setup and two cylinders arranged in tandem setup. A single-cylinder setup (Figure 1) is used for the validation study and the benchmark. Cartesian grid measurement is used for the domain size in this setup.

The size of the domain, length  $L/D$  and height  $H/D$ , will be 32 units and 16 units, respectively, and the diameter of the cylinder is 0.5 units. The position of the cylinder is located at coordinate (8, 8) of the domain. Note that the dimensions are measured as in the cartesian grid unit. The complete schematic of the setup is shown in Figure 1.

Boundary conditions of the computational domain are imposed as zero gradients for top and bottom walls. At inlet uniform velocity, a uniform velocity in the direction normal to the inlet is applied, while at the outlet, the pressure is set to zero-gauge pressure. The flow is incompressible in a two-dimensional configuration.

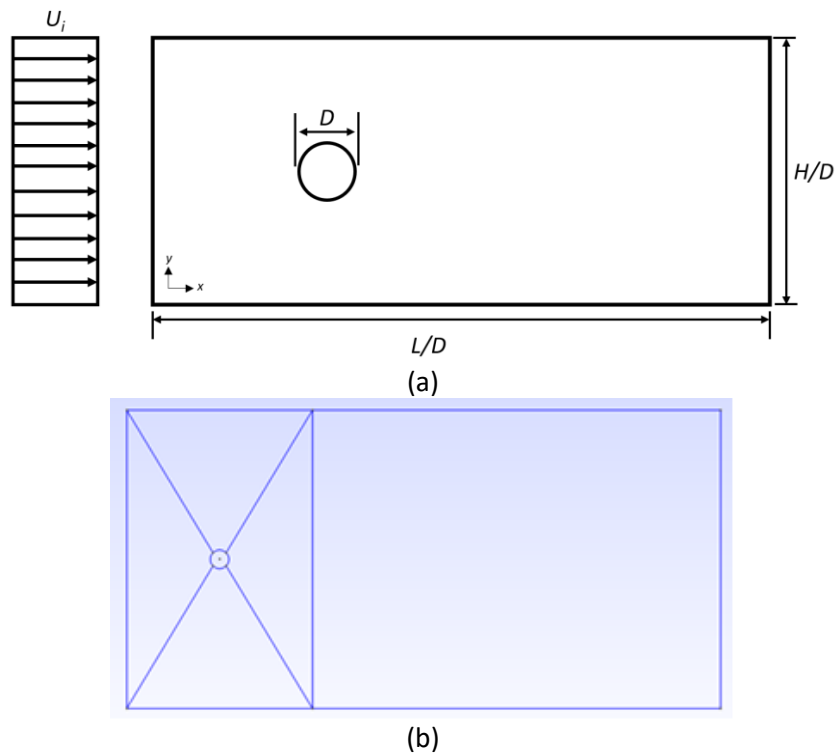


**Fig. 1.** The single-cylinder bluff body configuration (a) schematic drawing and (b) the drawing in *Gmsh*

The second setup will be two circular cylinders with an in-line or tandem arrangement (Figure 2). The size of the domain for two circular cylinders setup will be the factor of the diameter. The diameter,  $D$  of both cylinders is set at 1 unit.

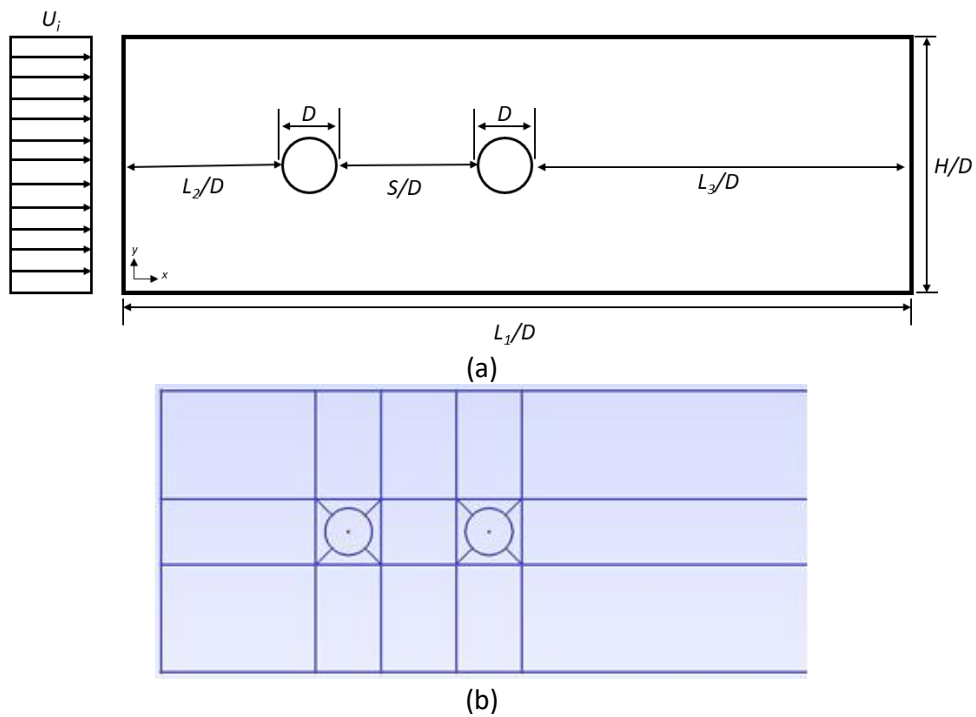


**Fig. 2.** The two-cylinders setup (a) schematic diagram and (b) the drawing in *Gmsh*

Compared to the single-cylinder configuration, the only differences are the domain size, and there is gap length between the two cylinders that are required to be fixed. The complete schematic of the configuration is shown in Figure 2. The gap length between the cylinder is given by  $S$ , where the length is the factor of the cylinder diameter. For the current study, several gap lengths are studied, which are  $2D$ ,  $3D$ ,  $4D$  and  $5D$ . The entry length is given by  $L_2$ , and the exit length is given by  $L_3$  are also by the factor of cylinder diameter and with fixed length where  $L_2 = 4D$  and  $L_3 = 20D$ .

Although *OpenFOAM* requires dimension, the current study analysis is based on nondimensional parameters. The present study will simulate these two cases of cylinder arrangement, namely a single cylinder and two cylinders in a tandem arrangement, with different Reynolds numbers ranging from 200 to 1000.

## 2.2 Meshing

The mesh structure was generated in *Gmsh*. The mesh for one and two cylinders are shown in Figure 3 and Figure 4, respectively. The mesh around the cylinders, especially behind the cylinder where the wake of the flow will appear, is enhanced by increasing the nodes on that particular region (refer to Figure 5). This is to ensure an accurate result and better post-processing analysis.

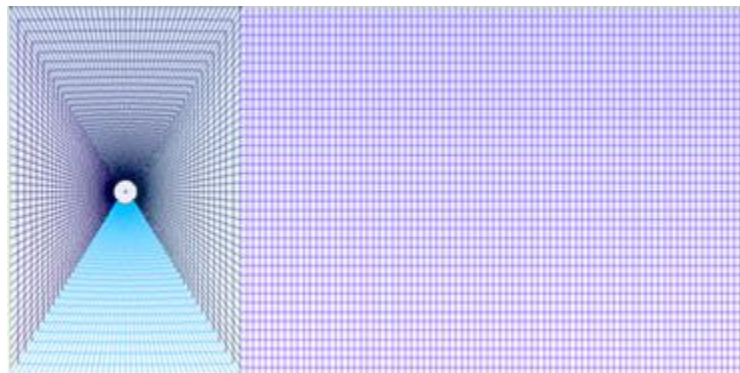


Fig. 3. Mesh structure for single cylinder setup

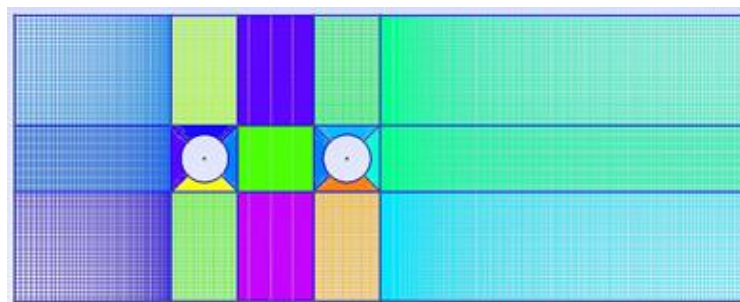


Fig. 4. Mesh structure for two cylinders set up

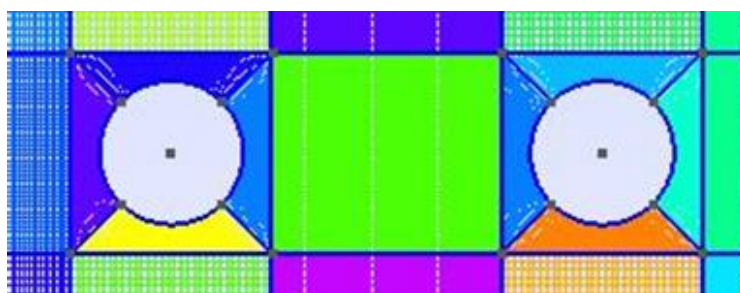


Fig. 5. Enhanced structured mesh around the cylinders

### 3. Results

#### 3.1 Validation

A validation study is done based on Calhoun's [19] report. This validation is conducted for a single-cylinder in a viscous crossflow problem. The response of the lift coefficient on the cylinder is studied with a laminar flow of  $Re = 100$ . The lift coefficient is a nondimensional quantity as a function of the force acting in the transverse ( $y$ ) direction,  $F_y$  (Eq. (5)). For a VIV at a low Reynolds number, the excitations behind a cylinder are very common to achieve, and the body-wake structure is similar as obtained by Blackburn and Henderson [13]. The simulation result is compared to three previous works, which are from the works of Braza *et al.*, [20], Calhoun [19] and Liu *et al.*, [21]. The comparison is listed in Table 1.

$$C_L = \frac{2F_y}{\rho U^2 D} \quad (5)$$

**Table 1**

Lift coefficient in comparison with past papers ( $\pm$  is the amplitude oscillation)

$Re = 100$	
Published Data	Lift coefficient ( $C_L$ )
Braza <i>et al.</i> , [20]	$\pm 0.250$
Calhoun [19]	$\pm 0.298$
Liu <i>et al.</i> , [21]	$\pm 0.339$
Present	$\pm 0.275$

#### 3.2 Grid Convergence Study

A grid convergence study is required to determine any discretisation error in CFD simulation. A convergence study is done with a single-cylinder case, and the objective is to observe any significant difference in results that could lead to error. Three cases are prepared: the reference case, increased domain size, and increased mesh resolution or nodes. These three cases were simulated for  $Re = 500$  and 600, and the Strouhal number and lift coefficient were observed.

There are minor differences between the two cases shown in Table 2 and Table 3. Therefore, the discretisation error can be neglected.

**Table 2**

Grid convergence study results and differences at  $Re=500$

$Re = 500$		
Published Data	Strouhal Frequency	Lift coefficient ( $C_L$ )
Refined 2D mesh (reference case)	0.001024	0.1362
Increase in domain size ( $h = 10D$ )	0.001138	0.1335
Increase in mesh resolution (nodes = 1.2)	0.001142	0.1339
Difference (%)	<11	<2

**Table 3**

Grid convergence study results and differences at  $Re=600$

$Re = 600$		
Published Data	Strouhal Frequency	Lift coefficient ( $C_L$ )
Refined 2D mesh (reference case)	0.001024	0.1441
Increase in domain size ( $h = 10D$ )	0.001165	0.1413
Increase in mesh resolution (nodes = 1.2)	0.001163	0.1424
Difference (%)	<14	<2

### 3.3 Lift Coefficient, Reynolds Number and Gap Length Relationship

The WIV response in this study is bounded by two parameters: the Reynolds number and the gap length between the two cylinders. The response analysis from the post-process results is studied over the harmonic response or the dominant response of the signal (Figure 6).

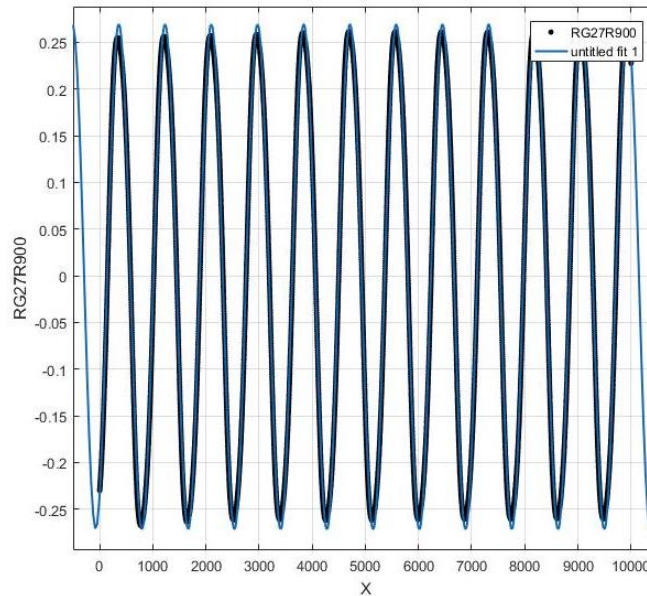


**Fig. 6.** The plot of time-history of lift coefficient on the downstream circular cylinder

The lift coefficient is representing the vertical force that is acting on the cylinder. The fluctuation of the lift force causes vibration to the cylinder. Therefore, it is desired to have a setup at the maximum lift coefficient. Furthermore, from a design point of view, a more compact structure is more convenient; thus, the smaller the gap length to obtain the maximum lift coefficient, the better the design is. Figure 7 showed that the gap length of  $2D$  and below would not produce a significant lift coefficient. The result showed that the lift coefficient over Reynolds number from all gap lengths of  $2D$  to  $5D$  showed an increasing pattern before reaching about a constant lift coefficient, except for the case of  $3D$  (Figure 7). There was a jump of lift coefficient between Reynolds number 300 and 400. Furthermore, as the gap length increase, the overall value of the lift coefficient is reducing. This indicates the minimum gap length value in producing the maximum lift coefficient between the gap length of  $2D$  and  $3D$ .

For further observation, the gap length is further increased from  $6D$  to  $10D$  to determine the behaviour over a longer gap between the two cylinders. The observation suggests that the lift coefficient shows a consistent trend in decrement as the gap length increases (Figure 8).

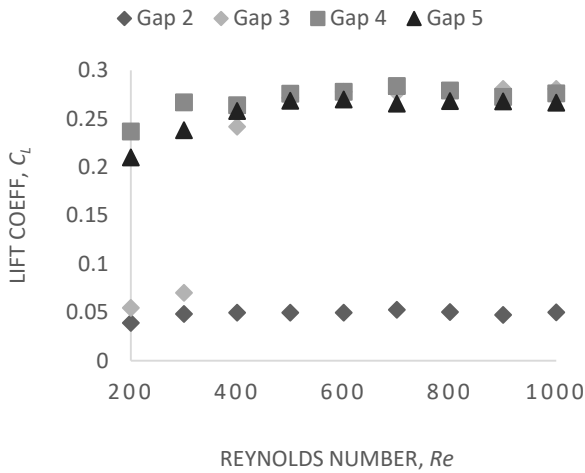


**Fig. 7.** Lift coefficient over Reynolds number for Gap=2D, 3D, 4D and 5D

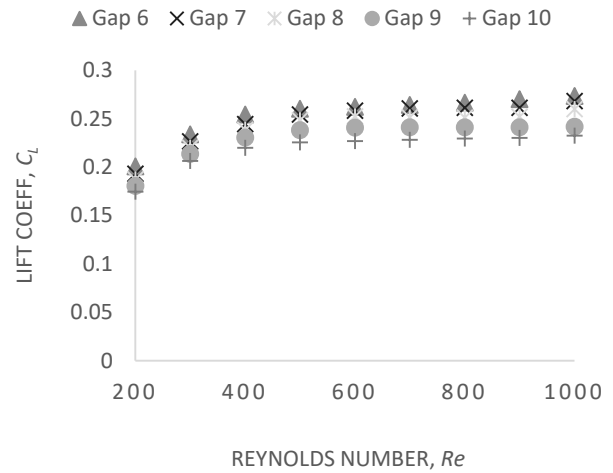


**Fig. 8.** Lift coefficient over Reynolds number for extended observation at Gap = 6D, 7D, 8D, 9D and 10D

The lift coefficient with gap length ranging from  $2.1D$  to  $2.9D$  was recorded. From the results, the highest value recorded for lift coefficient is located at a gap length of  $2.5D$  with a Reynolds number of 1000 (Table 4).

**Table 4**

Lift coefficient for gap length of  $2.1D$  to  $2.9D$  at  $Re = 1000$  with highest lift coefficient at  $2.5D$

$Re = 1000$	
Gap Length, $S$	Lift coefficient ( $C_L$ )
$2.1D$	0.05385
$2.3D$	0.04077
$2.5D$	0.30700
$2.7D$	0.27050
$2.9D$	0.27000

Figure 9 showed lift coefficient behaviour over Reynolds number. There is a significant 'jump' of the lift coefficient from  $Re = 500$  to  $600$  before the values decrease at  $Re = 700$ . Then, the lift coefficient is steadily increased from  $Re = 700$  to  $1000$  where the highest amplitude is recorded.

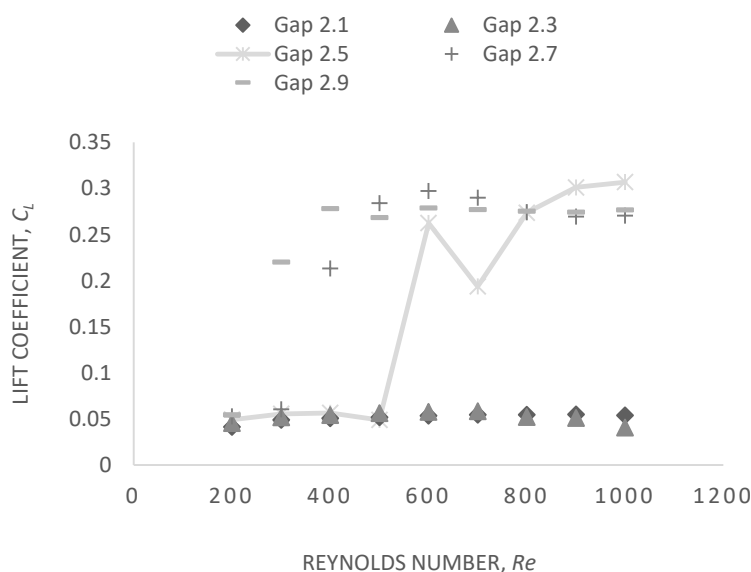


**Fig. 9.** Lift coefficient over Reynolds number for Gap = 2.1D to 2.9D with highest lift coefficient at 2.5D,  $Re = 1000$  (dash line)

It can be concluded that for a WIV design to obtain the maximum lift coefficient, the suitable gap length is located between the gap length of 2D and 3D. If the flow condition has a Reynolds number of 1000, then the optimal gap length is 2.5D.

### 3.4 VIV and WIV Comparison

A comparison is made between VIV and WIV responses to observe the difference. The domain dimension for both cases was set to be the same. The diameter of all cylinders also was set to be the same, which is 1 unit. The only difference between the two cases is the number of cylinders involved. With Reynolds numbers ranging from 200 to 1000, the response of the single-cylinder on the lift coefficient was observed.

The trend of the average lift coefficient of WIV for gap length 2D to 2.3D is observed lower than VIV (Figure 10). However, the average lift coefficient keeps increasing until it surpasses the lift coefficient of VIV on all tested Reynolds numbers ( $Re = 200$  to 1000) at gap lengths 4D and 5D (Figure 11). The lift coefficient showed an increasing pattern as the gap length increases. In between gap lengths 2.3D to 4D, the average lift coefficient shows unsteady values. The lift coefficient is lower than VIV at  $Re = 200, 300, 400$  and 500 for most of the gap lengths. The unsteadiness indicates the transition phase from gap length 2.4D to 3D (Figure 12).

In an extended observation, where the gap length is set to 15D to 17D, it is observed that the lift coefficient of the WIV case starts to act similar to the VIV case (Figure 13). The lift coefficient gradually decreases as it approaches the same values as in the VIV due to the big gap between the cylinders where the vortex formed behind the upstream cylinder starts to break and forms a steady uniform flow.

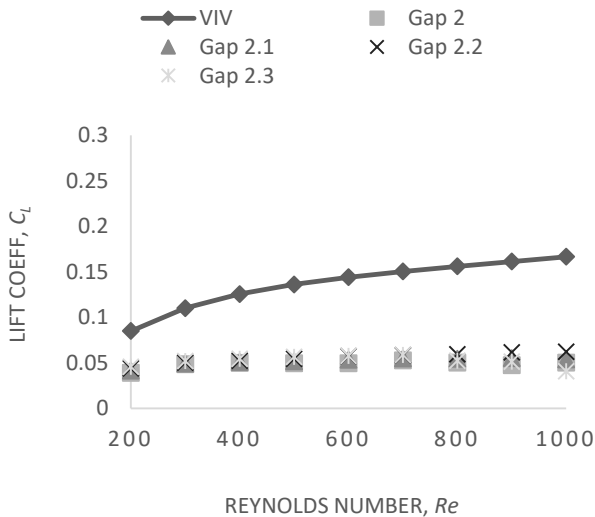


**Fig. 10.** WIV and VIV (dashed line) vs Re at Gap Length between 2D until 2.3D

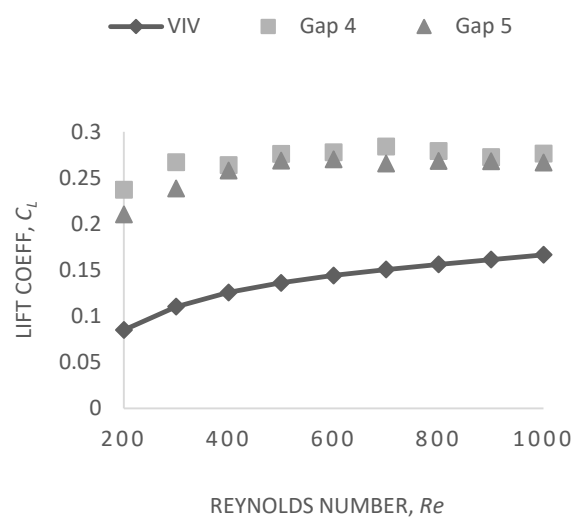


**Fig. 11.** WIV and VIV (dashed line) vs Re at Gap Length between 4D until 5D

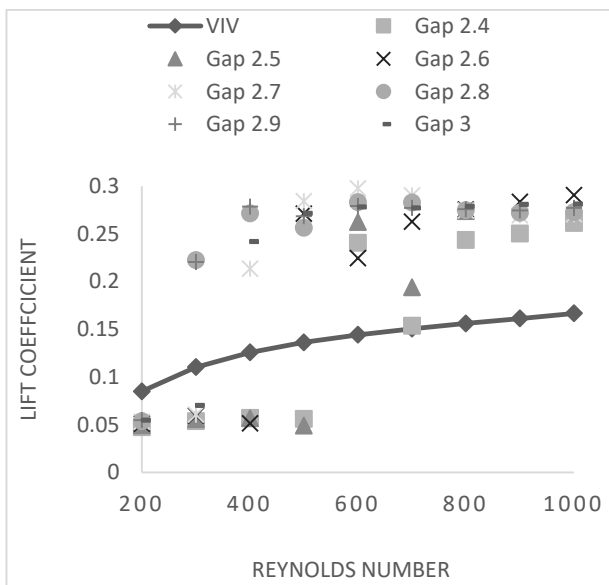


**Fig. 12.** WIV and VIV (dashed line) vs Re at Gap Length between 2.4D and 3D

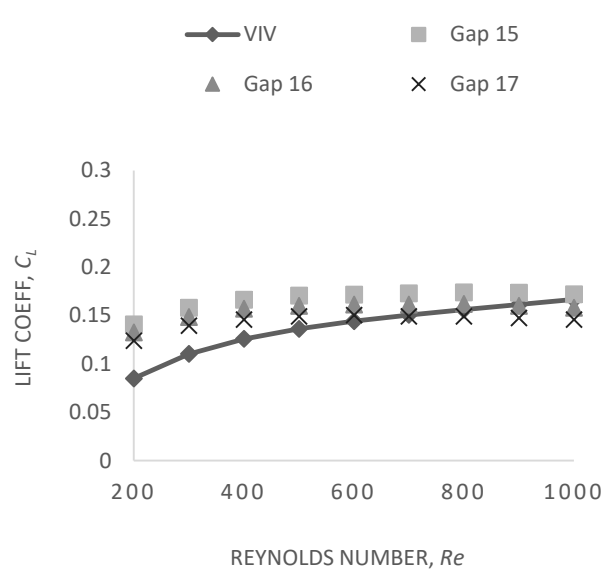


**Fig. 13.** WIV and VIV (dashed line) vs Re at Gap Length between 15D and 17D

From the observation, WIV can produce higher lift amplitude than VIV, with the values almost doubled than VIV case. The upstream cylinder acts as a vortex promoter to the downstream cylinder, where the lift coefficient is multiplied as it interacts with the downstream cylinder.

### 3.5 Strouhal-Reynolds Number Relationship

The Strouhal number and Reynolds number relationship are studied on gap length  $2.5D$  to  $10D$  with  $Re = 300, 500, 600$  and  $1000$ . The dimensionless frequency of the vortex formation behind the downstream cylinder shows different behaviours in different gap lengths and Reynolds numbers.

From the plotted Strouhal number versus gap length, the trend can be easily predicted. The Strouhal number is low on a lower Reynolds number and keeps increasing as the Reynolds number increases (Figure 14). This indicates that the vortex formation becomes more frequent as the external

flow becomes more vigorous as the Reynolds number increases. The trends also are similar in each gap length case.

In a further observation of Figure 14, on gap length  $4D$  to  $10D$ , a steady value of Strouhal number is observed. The Strouhal number is, however, independent of the gap length as the gap length increased further.

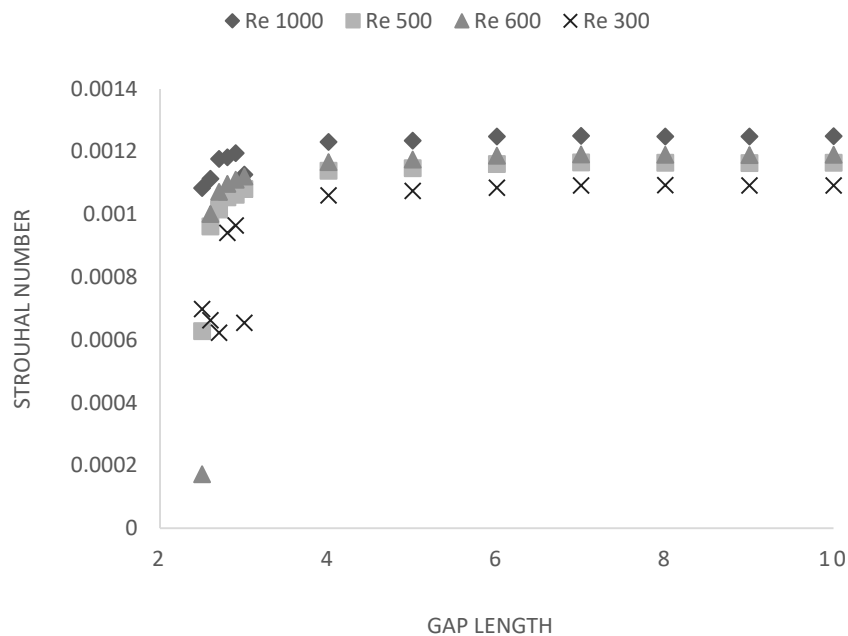


**Fig. 14.** Strouhal-Reynolds relationship on the effect of gap length with an asymptotic trend

#### 4. Conclusions

To conclude, the present study primarily investigates the behaviour and response of the external flow when interacting with two circular cylinders in a tandem arrangement in an external flow. From the observation of the results, there is an optimal gap length between the two cylinders with an optimal Reynolds number. At gap length  $2.5D$  with  $Re = 1000$ , the lift coefficient is at the highest value. This study provides the relationship between the Reynolds number and the gap length with the Strouhal number, which could provide insight into optimising WIV electricity generation. The Strouhal number shows an increase in trend while the Reynolds number and gap length increases. However, the Strouhal number is independent of gap length as the gap length is larger than  $6D$ .

#### Acknowledgement

This research was funded by a grant from IIUM-UMP-UiTM Sustainable Research Collaboration Grant 2020 (SRCG20-034-0034).

#### References

- [1] Chen, Shoei-Sheng. *Flow-induced vibration of circular cylindrical structures*. No. ANL-85-51. Argonne National Lab.(ANL), Argonne, IL (United States), 1985.
- [2] Pettigrew, M. J., C. E. Taylor, N. J. Fisher, M. Yetisir, and B. A. W. Smith. "Flow-induced vibration: recent findings and open questions." *Nuclear Engineering and Design* 185, no. 2-3 (1998): 249-276. [https://doi.org/10.1016/S0029-5493\(98\)00238-6](https://doi.org/10.1016/S0029-5493(98)00238-6)

- [3] Irwin, Peter A., Stoyan Stoyanoff, Jiming Xie, and Mark Hunter. "Tacoma Narrows 50 years later-wind engineering investigations for parallel bridges." *Bridge Structures* 1, no. 1 (2005): 3-17. <https://doi.org/10.1080/1573248042000274551>
- [4] Assi, GR da S., J. R. Meneghini, J. A. P. Aranha, P. W. Bearman, and E. Casaprima. "Experimental investigation of flow-induced vibration interference between two circular cylinders." *Journal of Fluids and Structures* 22, no. 6-7 (2006): 819-827. <https://doi.org/10.1016/j.jfluidstructs.2006.04.013>
- [5] Naseer, Rashid, Huliang Dai, Abdessattar Abdelkefi, and Lin Wang. "Comparative study of piezoelectric vortex-induced vibration-based energy harvesters with multi-stability characteristics." *Energies* 13, no. 1 (2020): 71. <https://doi.org/10.3390/en13010071>
- [6] Pinar, Engin, Tahir Durhasan, Göktürk M. Ozkan, Muhammed M. Aksoy, Huseyin Akilli, and Besir Sahin. "The effects of perforated cylinders on the vortex shedding on the suppression of a circular cylinder." In *EPJ Web of Conferences*, vol. 143, p. 02094. EDP Sciences, 2017. <https://doi.org/10.1051/epjconf/201714302094>
- [7] Soti, Atul Kumar, Mark C. Thompson, John Sheridan, and Rajneesh Bhardwaj. "Harnessing electrical power from vortex-induced vibration of a circular cylinder." *Journal of Fluids and Structures* 70 (2017): 360-373. <https://doi.org/10.1016/j.jfluidstructs.2017.02.009>
- [8] Zahari, M. A., and S. S. Dol. "Effects of different sizes of cylinder diameter on vortex-induced vibration for energy generation." *Journal of Applied Sciences* 15, no. 5 (2015): 783-791. <https://doi.org/10.3923/jas.2015.783.791>
- [9] Atrah, Ahmed B., Mohd Syuhaimi Ab-Rahman, Hanim Salleh, Mohd Zaki Nuawi, Mohd Jailani Mohd Nor, and Nordin Bin Jamaludin. "Karman vortex creation using cylinder for flutter energy harvester device." *Micromachines* 8, no. 7 (2017): 227. <https://doi.org/10.3390/mi8070227>
- [10] Assi, Gustavo R. S. "Wake-induced vibration of tandem cylinders of different diameters." *Journal of Fluids and Structures* 50 (2014): 329-339. <https://doi.org/10.1016/j.jfluidstructs.2014.07.001>
- [11] Assi, Gustavo R. S., P. W. Bearman, and J. R. Meneghini. "On the wake-induced vibration of tandem circular cylinders: the vortex interaction excitation mechanism." *Journal of Fluid Mechanics* 661 (2010): 365-401. <https://doi.org/10.1017/S0022112010003095>
- [12] Zhang, Min, and Junlei Wang. "Experimental study on piezoelectric energy harvesting from vortex-induced vibrations and wake-induced vibrations." *Journal of Sensors* 2016 (2016). <https://doi.org/10.1155/2016/2673292>
- [13] Blackburn, Hugh, and Ron Henderson. "Lock-in behavior in simulated vortex-induced vibration." *Experimental Thermal and Fluid Science* 12, no. 2 (1996): 184-189. [https://doi.org/10.1016/0894-1777\(95\)00093-3](https://doi.org/10.1016/0894-1777(95)00093-3)
- [14] Fu, Yingnan, Xizeng Zhao, Xinggang Wang, and Feifeng Cao. "Computation of flow past an in-line oscillating circular cylinder and a stationary cylinder in tandem using a CIP-based model." *Mathematical Problems in Engineering* 2015 (2015). <https://doi.org/10.1155/2015/568176>
- [15] Singh, S. P., and G. Biswas. "Vortex induced vibrations of a square cylinder at subcritical Reynolds numbers." *Journal of Fluids and Structures* 41 (2013): 146-155. <https://doi.org/10.1016/j.jfluidstructs.2013.03.011>
- [16] Parsons, Stuart, and Phil Battley. "Impacts of wind energy developments on wildlife: a southern hemisphere perspective." *New Zealand Journal of Zoology* 40, no. 1 (2013): 1-4. <https://doi.org/10.1080/03014223.2012.758156>
- [17] Wang, Junlei, Linfeng Geng, Lin Ding, Hongjun Zhu, and Daniil Yurchenko. "The state-of-the-art review on energy harvesting from flow-induced vibrations." *Applied Energy* 267 (2020): 114902. <https://doi.org/10.1016/j.apenergy.2020.114902>
- [18] Kazim, Mohd Nor Fakhzan Mohd, Rasidi Rasani, Mohd Zaki Nuawi, Zamri Harun, Yap Khang Hau, and Mohd Shukry Abdul Majid. "Analysis of wake region behind bluff body for piezoelectric energy harvester." *Journal of Advanced Research in Fluid Mechanics and Thermal Sciences* 55, no. 2 (2019): 249-263.
- [19] Calhoun, Donna. "A Cartesian grid method for solving the two-dimensional streamfunction-vorticity equations in irregular regions." *Journal of Computational Physics* 176, no. 2 (2002): 231-275. <https://doi.org/10.1006/jcph.2001.6970>
- [20] Braza, M., P. H. H. M. Chassaing, and H. Ha Minh. "Numerical study and physical analysis of the pressure and velocity fields in the near wake of a circular cylinder." *Journal of Fluid Mechanics* 165 (1986): 79-130. <https://doi.org/10.1017/S0022112086003014>
- [21] Liu, C., X. Zheng, and C. H. Sung. "Preconditioned multigrid methods for unsteady incompressible flows." *Journal of Computational Physics* 139, no. 1 (1998): 35-57. <https://doi.org/10.1006/jcph.1997.5859>